The role of magnetic field topology in core-collapse supernovae

Matteo Bugli[1]

Collaborators: J. Guilet[1], R. Raynaud[1], A. Reboul-Salze[1], M. Obergaulinger[2,3], P. Cerdà-Duràn[3],M. À. Aloy[3]

[1]Astrophysics Department, IRFU/CEA-Saclay, Gif-sur-Yvette, Paris
[2]Theoriezentrum, Technische Universität Darmstadt
[3]Departament d'Astronomia i Astrofisica, Universiat de València

Cosmic Explosions - Cargese, 29$^{\text{th}}$ May 2019

Core-collapse Supernovæ

- gravitational collapse of a massive star (unstable iron core)
- shock formation when nuclear densities are reached (stalling)
- shock expansion and ejection of unbound material (explosion)
- Key feature: revival of the stalling shock.

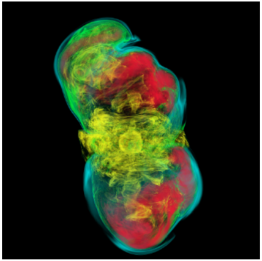

Mösta et al. (2014)

Neutrino-heating mechanism

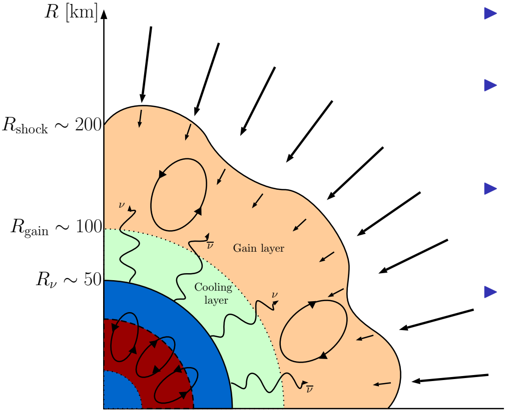

- PNS contraction ⇒ higher ν energies
- ν-cooling rate drops faster than ν-heating ⇒ Gain radius
- Energy deposition by ν_e and $\bar{\nu}_e$ absorption in gain layer
- Multi-D hydrodynamic instabilities aid the explosion (i.e. convection, SASI)

CCSN and magnetic fields

- Kinetic energies: 10^{51} ergs; rare Hypernovæ/LGRBs $\sim 10^{52}$ ergs
- Luminosities: 10^{49} ergs; Superluminous SN $\sim 10^{51}$ ergs.
- Need for extra energy reservoir $\Rightarrow$ rotation and magnetic fields of a millisecond magnetar? (Burrows et al., 2007; Bucciantini et al., 2009; Metzger et al., 2011; Takiwaki et al., 2009; Takiwaki and Kotake, 2011; Obergaulinger and Aloy, 2017)

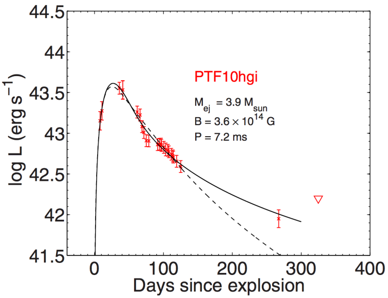

(Inserra et al., 2013)

The ERC-MagBurst project

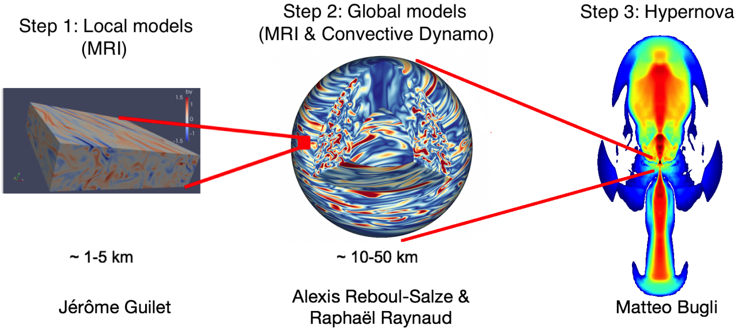

- Amplification of magnetic field and magnetar formation
- Multi-scale problem, interconnected steps
- Complex topologies produced by dynamos in the PNS, not just dipoles!

The progenitor: 35OC (Woosley and Heger, 2006)

- $M_{ZAMS} = 35 M_{\odot}$, mass at collapse $\sim 28 M_{\odot}$
- Iron core of $\sim 2.1 M_{\odot}$, surrounded by $\sim 4 M_{\odot}$ of convective zone
- Original rotation profile from stellar evolution, rapid rotation

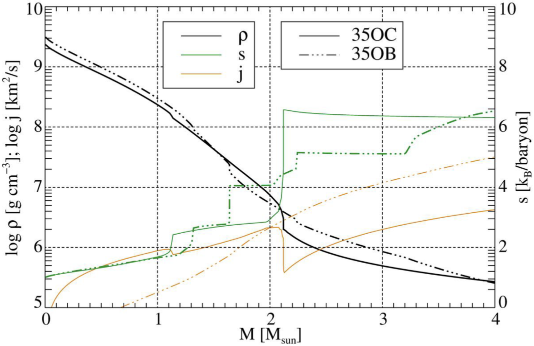

Comparison: different multipoles (Bugli et al., in prep.)

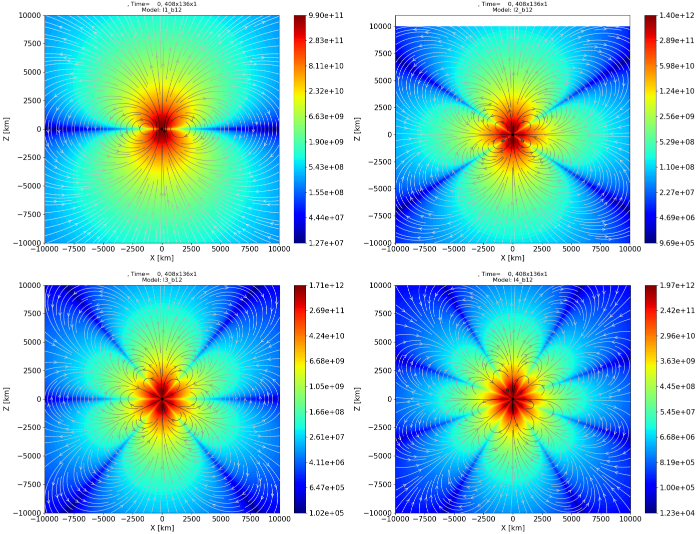

Onset of the explosion $(r_0 = 2.9 \times 10^8\text{cm}, B_0 = 8 \times 10^{10}\text{G})$

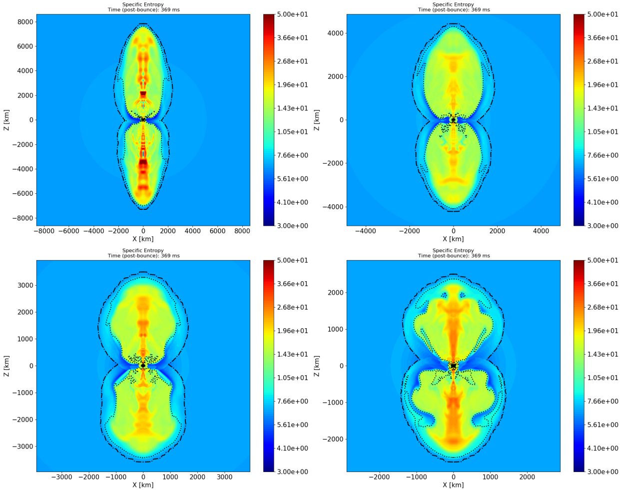

Shock radii ($r_0 = 2.9 \times 10^8$cm, $B_0 = 8 \times 10^{10}$G)

- Onset of explosion onset at the same time
- Slower expansion for higher multipoles

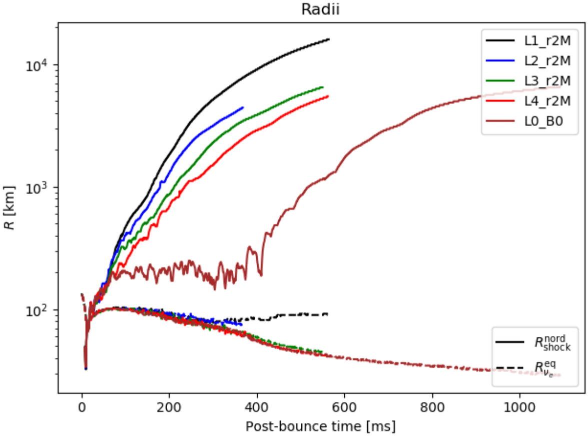

Explosion energy $(r_0 = 2.9 \times 10^8\text{cm}, B_0 = 8 \times 10^{10}\text{G})$

- Less energetic explosion and shallower increase of energy for higher multipoles

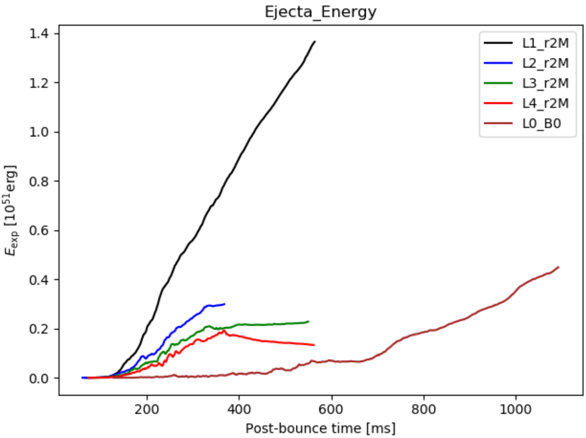

Magnetic/thermal pressure ($r_0 = 2.9 \times 10^8$cm, $B_0 = 8 \times 10^{10}$G)

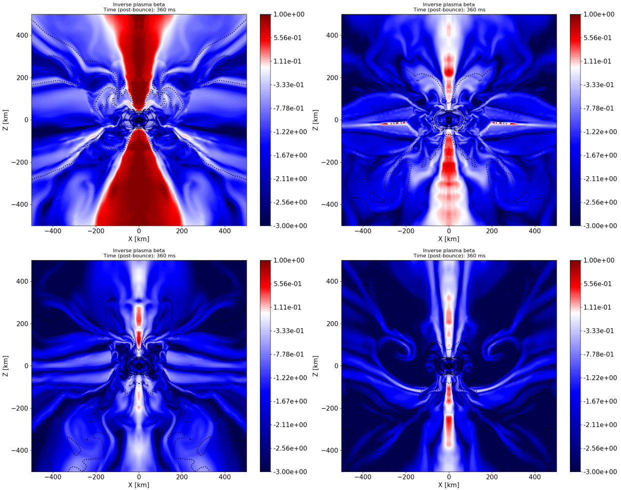

$l = 1$ vs $l = 4$ ($r_0 = 2.9 \times 10^8$cm, $B_0 = 8 \times 10^{10}$G)

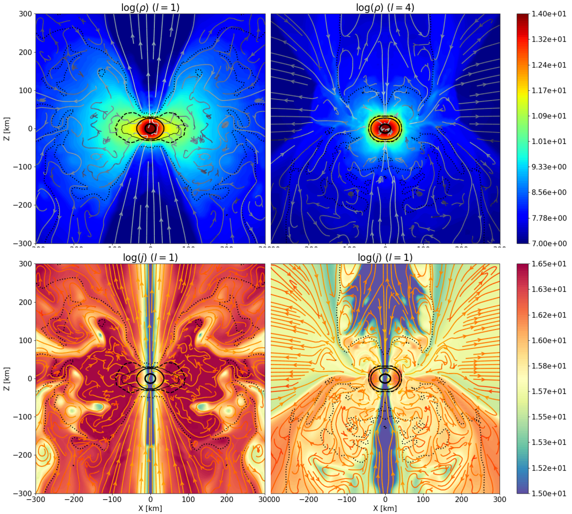

- mass density
- specific angular momentum

PNS mass and spin $(r_0 = 2.9 \times 10^8\text{cm}, B_0 = 2.6 \times 10^{11}\text{G})$

Higher multipole order $\Rightarrow$ closer to hydrodynamic limit:

- faster increase of total angular momentum (weaker magnetic braking)
- faster increase of total mass

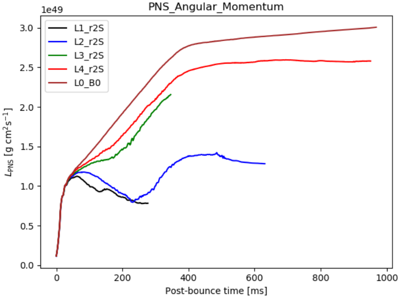

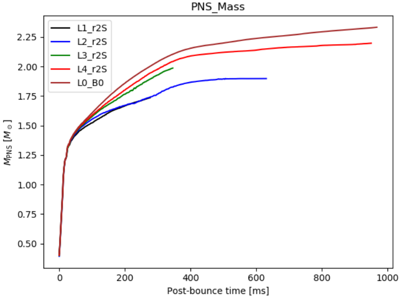

Conclusions

- Different multipolar configurations have a strong impact on the explosion dynamics: higher $l \Rightarrow$ less energetic (delayed) explosion, less collimated ejecta
- Impact on the PNS formation:
  - less oblate surface, different Y_e distribution
  - shallower distribution of angular momentum
  - faster rotation, more massive PNS
- Radial extent of the magnetic field can also affect the dynamics (different degree of compression)

Perspectives

- Extension to later times
- Extension to 3D using the axisymmetric models as guiding line
- Subgrid modeling of the unresolved dynamo in the PNS (mean-field approach?)


Grazia per a vostra attenzione!

References I

Ardeljan, N. V., Bisnovatyi-Kogan, G. S., and Moiseenko, S. G. (2005). Magnetorotational supernovae. *Monthly Notices of the Royal Astronomical Society*, 359(1):333.

Blandford, R. D. and Znajek, R. L. (1977). Electromagnetic extraction of energy from Kerr black holes. *\mnras*, 179:433–456.

Bucciantini, N., Quataert, E., Metzger, B. D., Thompson, T. A., Arons, J., and Del Zanna, L. (2009). Magnetized relativistic jets and long-duration GRBs from magnetar spin-down during core-collapse supernovae. *Monthly Notices of the Royal Astronomical Society*, 396:2038–2050.

Burrows, A., Dessart, L., Livne, E., Ott, C. D., and Murphy, J. (2007). Simulations of Magnetically Driven Supernova and Hypernova Explosions in the Context of Rapid Rotation. *The Astrophysical Journal*, 664(1):416.

References II

Dessart, L., Burrows, A., Livne, E., and Ott, C. D. (2008). The Proto-Neutron Star Phase of the Collapsar Model and the Route to Long-Soft Gamma-Ray Bursts and Hypernovae. *\apjl*, 673:L43.

Inserra, C., Smartt, S. J., Jerkstrand, A., Valenti, S., Fraser, M., Wright, D., Smith, K., Chen, T.-W., Kotak, R., Pastorello, A., Nicholl, M., Bresolin, F., Kudritzki, R. P., Benetti, S., Botticella, M. T., Burgett, W. S., Chambers, K. C., Ergon, M., Flewelling, H., Fynbo, J. P. U., Geier, S., Hodapp, K. W., Howell, D. A., Huber, M., Kaiser, N., Leloudas, G., Magill, L., Magnier, E. A., McCrum, M. G., Metcalfe, N., Price, P. A., Rest, A., Sollerman, J., Sweeney, W., Taddia, F., Taubenberger, S., Tonry, J. L., Wainscoat, R. J., Waters, C., and Young, D. (2013). Super-luminous Type Ic Supernovae: Catching a Magnetar by the Tail. *The Astrophysical Journal*, 770(2):128.

References III

Just, O., Obergaulinger, M., and Janka, H.-T. (2015). A new multidimensional, energy-dependent two-moment transport code for neutrino-hydrodynamics. *\mnras*, 453:3386–3413.

Metzger, B. D., Giannios, D., Thompson, T. A., Bucciantini, N., and Quataert, E. (2011). The protomagnetar model for gamma-ray bursts. *Monthly Notices of the Royal Astronomical Society*, 413(3):2031.

Metzger, B. D., Thompson, T. A., and Quataert, E. (2018). A magnetar origin for the kilonova ejecta in GW170817. *ArXiv e-prints*, 1801:arXiv:1801.04286.

Mösta, P., Richers, S., Ott, C. D., Haas, R., Piro, A. L., Boydstun, K., Abdikamalov, E., Reisswig, C., and Schnetter, E. (2014). Magnetorotational Core-collapse Supernovae in Three Dimensions. *The Astrophysical Journal*, 785(2):L29.

References IV

Obergaulinger, M. and Aloy, M. A. (2017). Evolution of the surface magnetic field of rotating proto-neutron stars. *Journal of Physics: Conference Series*, 932:012043.

Sawai, H., Kotake, K., and Yamada, S. (2005). Core-Collapse Supernovae with Nonuniform Magnetic Fields. *The Astrophysical Journal*, 631(1):446.

Spruit, H. C. (2002). Dynamo action by differential rotation in a stably stratified stellar interior. *Astronomy and Astrophysics*, 381:923.

Suwa, Y., Takiwaki, T., Kotake, K., and Sato, K. (2007). Magnetorotational Collapse of Population III Stars. *Publications of the Astronomical Society of Japan*, 59(4):771–785.

Takiwaki, T. and Kotake, K. (2011). GRAVITATIONAL WAVE SIGNATURES OF MAGNETOHYDRODYNAMICALLY DRIVEN CORE-COLLAPSE SUPERNOVA EXPLOSIONS. *The Astrophysical Journal*, 743(1):30.

References V

Takiwaki, T., Kotake, K., and Sato, K. (2009). Special Relativistic Simulations of Magnetically Dominated Jets in Collapsing Massive Stars. *ApJ*, 691(2):1360.

Tchekhovskoy, A. (2015). Launching of Active Galactic Nuclei Jets. In Contopoulos, I., Gabuzda, D., and Kylafis, N., editors, *The Formation and Disruption of Black Hole Jets*, Astrophysics and Space Science Library, pages 45–82. Springer International Publishing, Cham.

Tchekhovskoy, A., Narayan, R., and McKinney, J. C. (2011). Efficient generation of jets from magnetically arrested accretion on a rapidly spinning black hole. *\mnras*, 418:L79–L83.

Uzdensky, D. A. and MacFadyen, A. I. (2006). Stellar Explosions by Magnetic Towers. *The Astrophysical Journal*, 647(2):1192.

Woosley, S. E. (1993). Gamma-ray bursts from stellar mass accretion disks around black holes. *The Astrophysical Journal*, 405:273–277.

References VI

Woosley, S. E. and Heger, A. (2006). The Progenitor Stars of Gamma-Ray Bursts. *The Astrophysical Journal*, 637(2):914.

Relativistic outflows

- Magnetic fields are crucial in the launch and collimation of relativistic outflows (Blandford and Znajek, 1977; Uzdensky and MacFadyen, 2006; Tchekhovskoy et al., 2011).
- Key parameters: central object rotation, radial magnetic field flux.

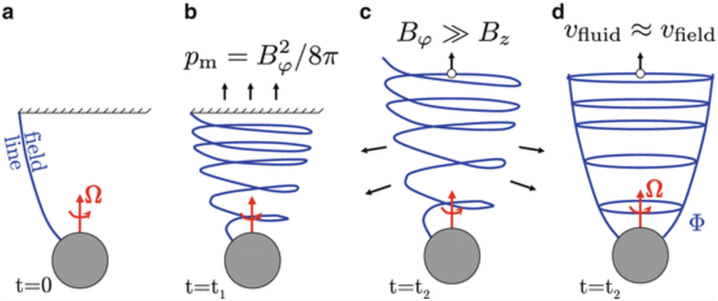

(Tchekhovskoy, 2015)

The Magnetar Model

- The evolution of the PNS spin and magnetic field regulates the dynamics of PNS wind and explosion: $\sigma = \frac{\dot{E}_{\rm mag} + \dot{E}_{\rm kin}}{\dot{M}c^2}$

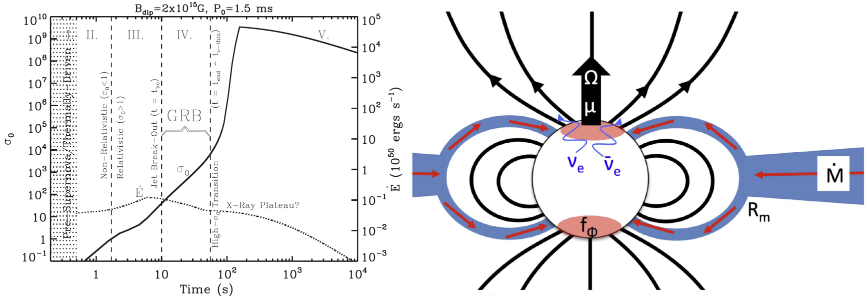

(Metzger et al., 2011, 2018)

Magnetar vs Collapsar

- Two possible scenarios for magnetic energy extraction:
  - Millisecond magnetar (Metzger et al., 2011)
  - Collapsar (Woosley, 1993)
- Massive progenitors do not necessarily lead to direct collapse (Dessart et al., 2008; Obergaulinger and Aloy, 2017)
- Understanding the accretion dynamics onto the PNS is crucial
- Successful explosions and collapse to BH may not be mutually exclusive
- Many uncertainties on the characteristics of magnetic field at shock formation:
  - From stellar progenitor or forming PNS?
  - Dipolar? Complex topology?

Sub-grid modeling of the PNS dynamo

- Fields amplified to magnetar-like strength ($10^{14} - 10^{15}$ G).
- Topology: non-dipolar fields produced by dynamos.
- Time evolution: delay between the bounce and the rise of the magnetic field.
- At what stages can the amplified field affect the shock revival?

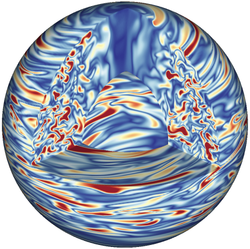

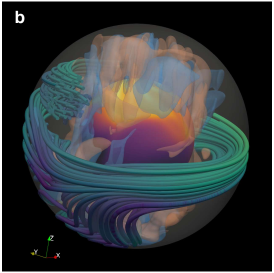

MRI and convection driven dynamos

Initial magnetic field: pure dipole?

- Poor constraints from both observations and evolutionary models on the initial field.
- Quasi-uniform field up to $r_0 \sim 10^3$km, then magnetic dipole (Suwa et al., 2007):

$$A_\phi = \frac{B_0}{2} \frac{r_0^3}{r^3 + r_0^3} r \sin\theta$$

- Progenitor *original* field from 1D stellar evolution (Woosley and Heger, 2006)
- Superimposed toroidal field (Obergaulinger and Aloy, 2017):

$$B_\phi = B_0 \frac{r_0^3}{r^3 + r_0^3} r \cos\theta$$

Quadrupole in the literature: contradicting results

Ardeljan et al. (2005)

- Magnetic field "turned on" after bounce
- Explosion energy: 0.6×10^{51} ergs
- Strong ejection along the equator

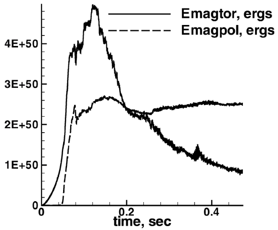

Sawai et al. (2005)

- Pre-collapse magnetic field
- Explosion energy: $(0.24 - 0.59) \times 10^{51}$ ergs
- More collimated and faster polar outflows

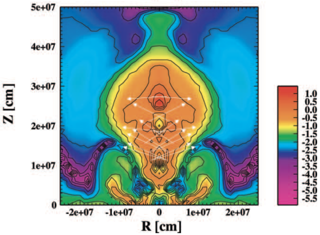

Numerical tool

- Multi-D relativistic MHD code ALCAR (Just et al., 2015)
- TOV gravity
- Multi-D M1-closure ν-transport
- Equation of State:
  - High density ($\rho > 10^7$g/cm^3): LS220
  - Low density ($\rho < 10^7$g/cm^3): photons, relativistic and degenerate e^- / e^+, non-relativistic baryons (^{28}Si for $T < 0.44$MeV, ^{56}Ni otherwise)
- High-order reconstruction schemes, angular coarsening

Initial magnetic field

- Not using the original magnetic fields from 1D stellar evolution model (Spruit, 2002)
- Generalized multipolar expansion:

$$A_{\phi,l} = B_0 \frac{\sqrt{l}}{2l+1} \frac{r_0^{l+2}}{r^{l+2} + r_0^{l+2}} r \frac{P_{l-1}(\cos\theta) - P_{l+1}(\cos\theta)}{\sin\theta}$$

- Radial magnetic field strength at the poles:

$$|\boldsymbol{B}_l(r, \theta = 0)| = \sqrt{l} \frac{B_0}{1 + (r/r_0)^{l+2}}$$

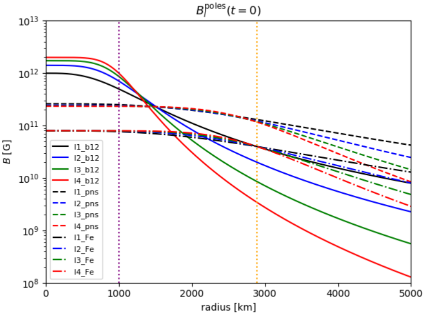

Models ($N_r = 400$, $N_\theta = 128$)(Bugli et al. 2019, in prep.)

	l	B_0 $[10^{10}\mathrm{G}]$	r_0 $[10^8\mathrm{cm}]$	E_{mag,r_0} $[10^{47}\mathrm{erg}]$
l1_PNS	1	26.1	2.89	10.9
l2_PNS	2	17.3	2.89	4.46
l3_PNS	3	13.7	2.89	2.91
l4_PNS	4	11.7	2.89	2.23
l1_Fe	1	7.97	2.89	1.02
l2_Fe	2	5.64	2.89	0.47
l3_Fe	3	4.60	2.89	0.33
l4_Fe	4	3.99	2.89	0.26
l1_b12	1	100	1	6.62
l2_b12	2	100	1	6.12
l3_b12	3	100	1	6.36
l4_b12	4	100	1	6.70

Shock radii ($r_0 = 10^8$cm, $B_0 = 10^{12}$G)

- Longer stalling phase for higher multipoles (faster radial decay)

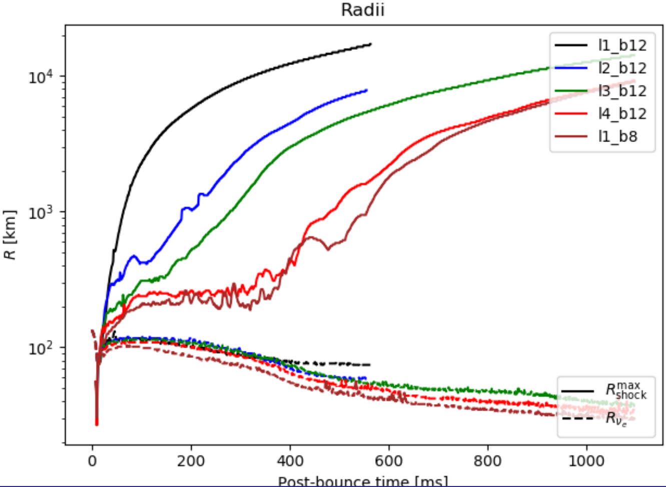

Explosion energy ($r_0 = 2.9 \times 10^8$cm, $B_0 = 2.6 \times 10^{11}$G)

- Less energetic explosion and shallower increase of energy for higher multipoles

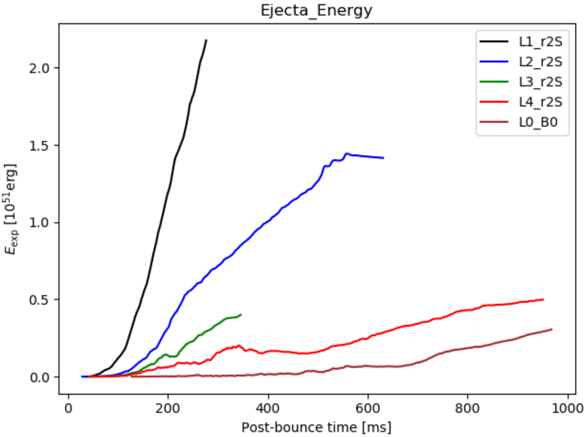

3D models

Qualitative differences between 2D and 3D magnetized models:

- wrong hydrodynamic turbulent cascade
- inhibition of non-axisymmetric instabilities: kink modes (Mösta et al., 2014)
- Cowling's anti-dynamo theorem

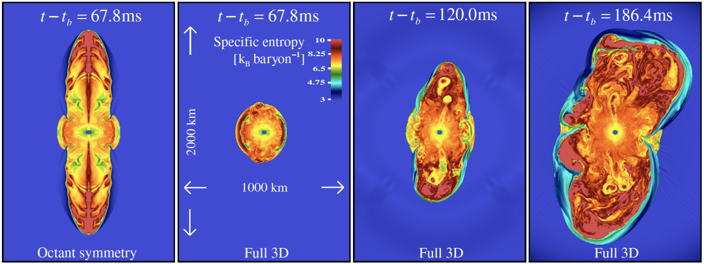

Y_e: $(l = 1)$ vs. $(l = 4)$ $(r_0 = 2.9 \times 10^8\text{cm}, B_0 = 8 \times 10^{10}\text{G})$

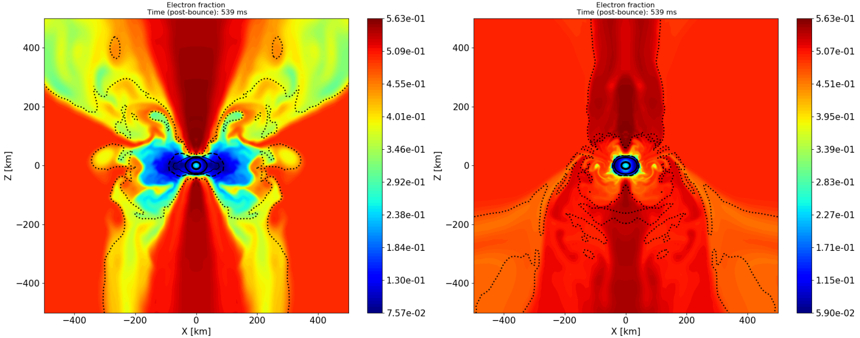

Neutrino luminosities along equator

More oblate PNS $\Rightarrow$ lower surface temperature $\Rightarrow$ less energetic ν

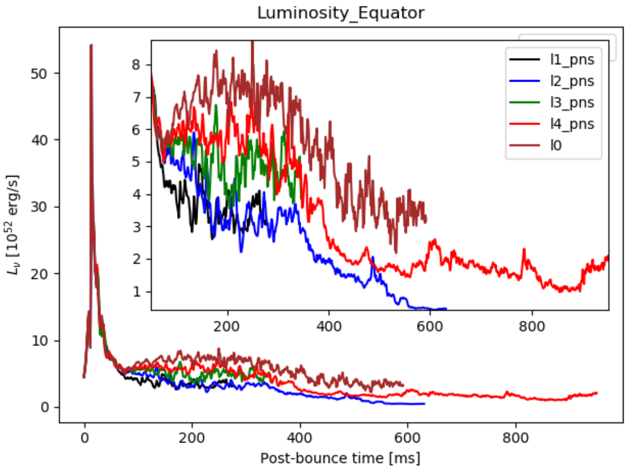

Baryon loading parameter (Magnetar model)

Dynamics of the outflow regulated by: $\sigma = \frac{\dot{E}_{\rm mag} + \dot{E}_{\rm kin}}{\dot{M}c^2}$

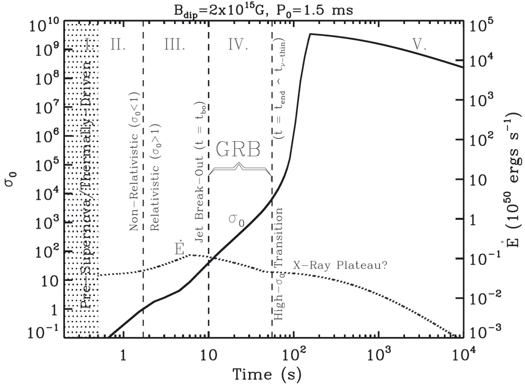

(Metzger et al., 2011)

Baryon loading parameter ($r_0 = 2.9 \times 10^8$cm, $B_0 = 8 \times 10^{10}$G)

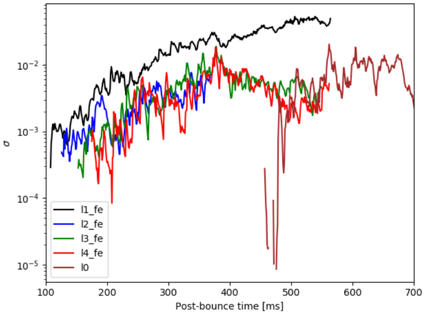

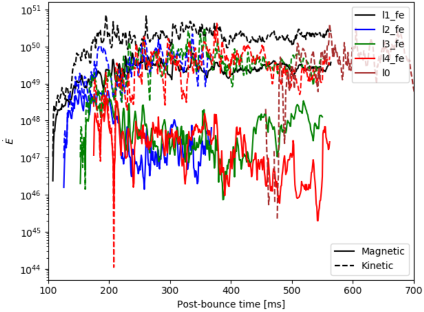

PNS magnetic energy ($r_0 = 2.9 \times 10^8$cm, $B_0 = 8 \times 10^{10}$G)

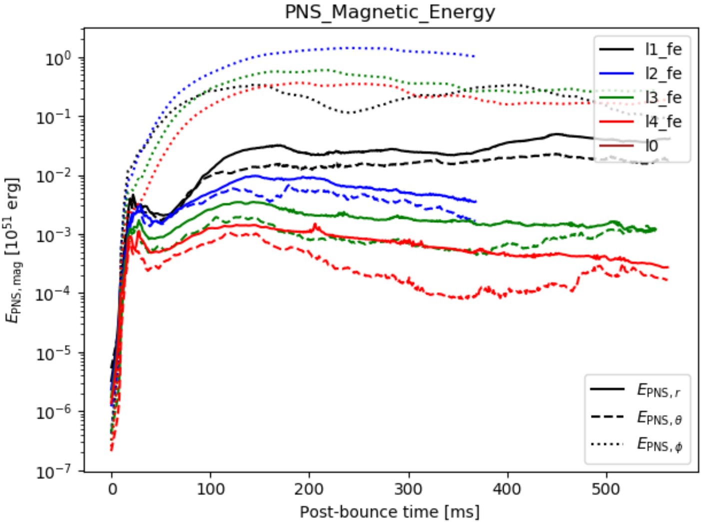

Harmonic distribution at $R_{\rm PNS}$ ($r_0 = 2.9 \times 10^8$cm, $B_0 = 8 \times 10^{10}$G)

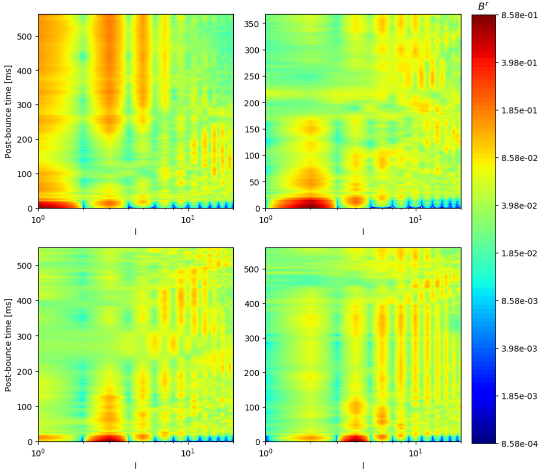

Radial magnetic field (time vs. multipole order)

Harmonic distribution at $R_{\rm PNS}$ ($r_0 = 2.9 \times 10^8$cm, $B_0 = 8 \times 10^{10}$G)

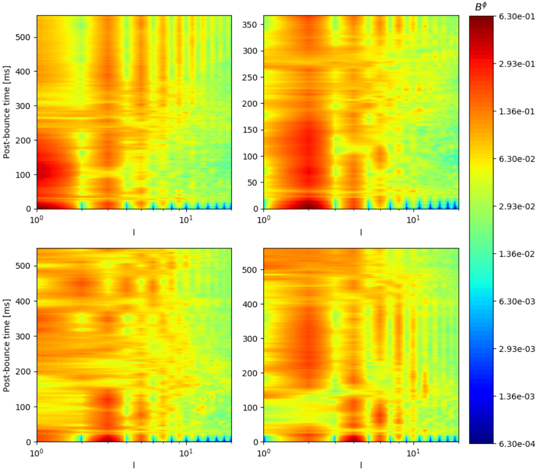

Azimuthal magnetic field (time vs. multipole order)